Electronic Supplementary Material (ESI) for Sustainable Energy & Fuels.
This journal is © The Royal Society of Chemistry 2022

Improving the electron transfer in oxygen reduction reaction by N/S co-doping for high-performance of Zn-air batteries

Jiawei Wei‡, Ping Li‡, Jing Shi, Minghua Huang, Weiqian Tian*, Huanlei Wang*

School of Materials Science and Engineering, Ocean University of China, Qingdao 266100, P.R. China.

E-mail: huanleiwang@gmail.com; tianweiqian@ouc.edu.cn

‡ These co-first authors contributed equally to this work.

Electrochemical measurements

The electron transfer numbers (*n*) were calculated by the K-L equations as follows

$$\frac{1}{j}=\frac{1}{j_L}+\frac{1}{j_K}=\frac{1}{B\omega^{0.5}}+\frac{1}{j_K}$$

$$B=0.62nFC_0D_0^{\frac{2}{3}}V^{-\frac{1}{6}}$$

where j is the measured current density, j_K and j_L are the kinetic and limiting current densities, ω is the angular velocity of the disk, n is the overall number of electrons transferred in oxygen reduction, F is the Faraday constant (96485 C mol^{-1}), C_0 is the bulk concentration of O_2 (1.2×10^{-6} mol cm^{-3}), D_0 is the diffusion coefficient of O_2 in 0.1 M KOH (1.9×10^{-5} cm^2 s^{-1}), and V is the kinematic viscosity of the electrolyte (0.01 cm^2 s^{-1}).

For the RRDE test, the disk electrode was scanned at a rate of 10 mV s^{-1} at a rotating speed of 1600 rpm, and the ring potential was kept at 1.4 V versus RHE. The peroxide percentage (H_2O_2%) and the electron transfer number (*n*) were determined by the following equations

$$H_2O_2=\frac{200\times I_r}{N\times I_d+I_r}$$

$$n=\frac{4\times I_d}{I_d+\frac{I_r}{N}}$$

where I_d is disk current, I_r is ring current, and N is current collection efficiency of the Pt ring. N was determined to be 0.37.

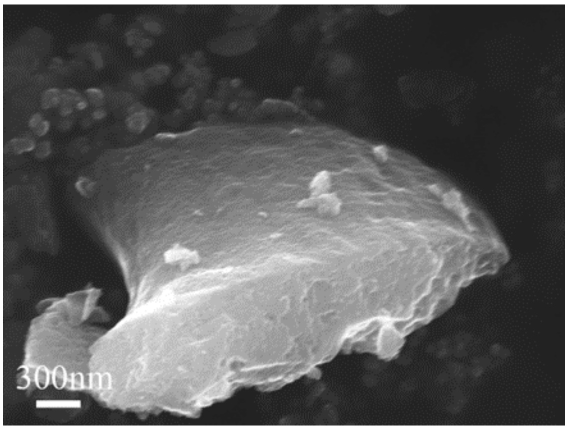

Fig. S1 SEM of NSC-800

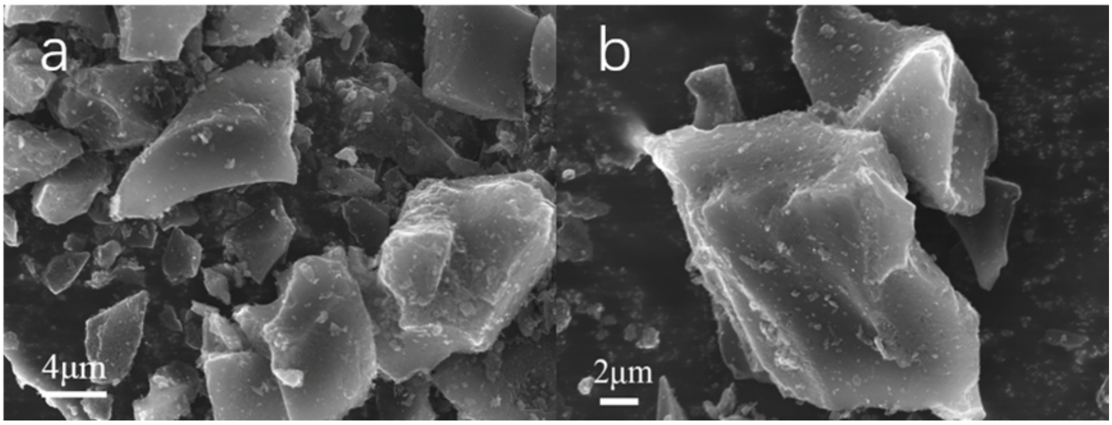

Fig. S2 SEM of SC-800

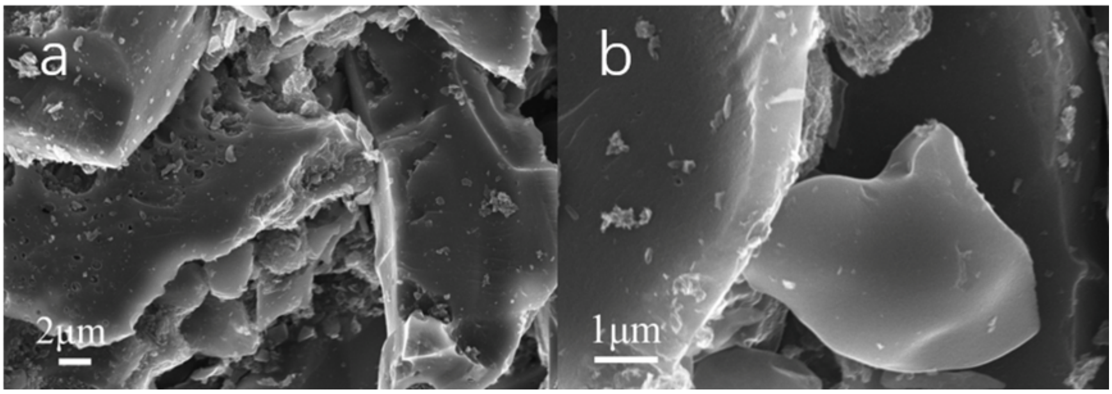

Fig. S3 SEM of NC-800

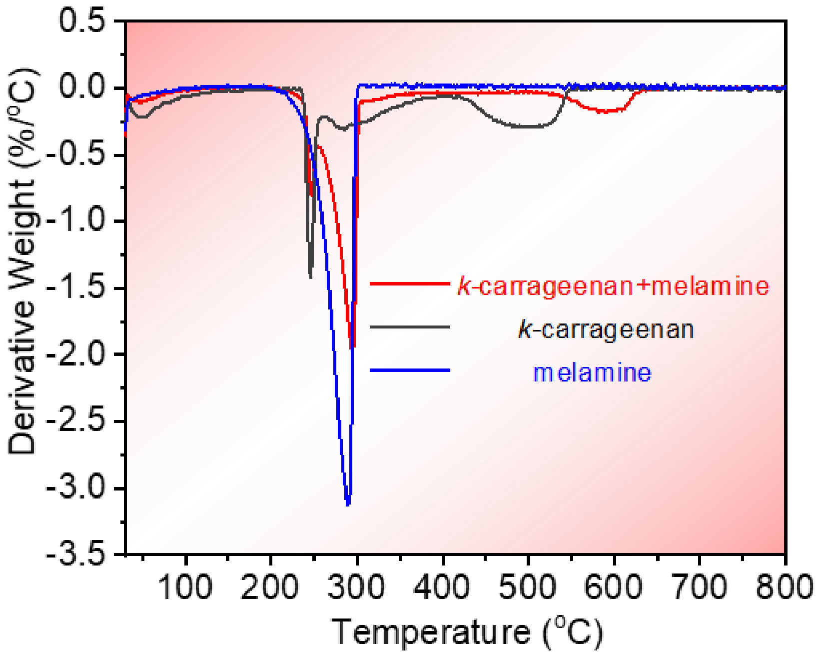

Fig. S4 DTG curves of carrageenan with melamine; carrageenan and melamine.

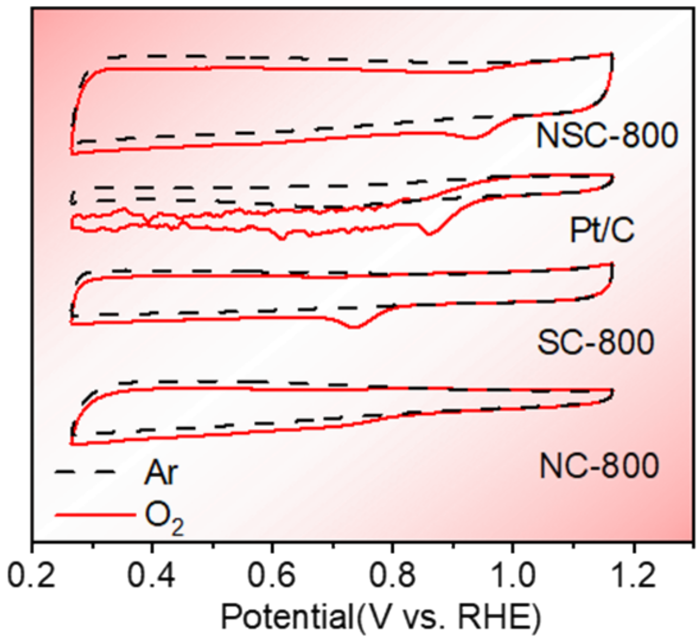

Fig. S5 CV tests for NSC-800, SC-800, NC-800, and Pt/C under Ar and O_2 saturated 0.1 m KOH.

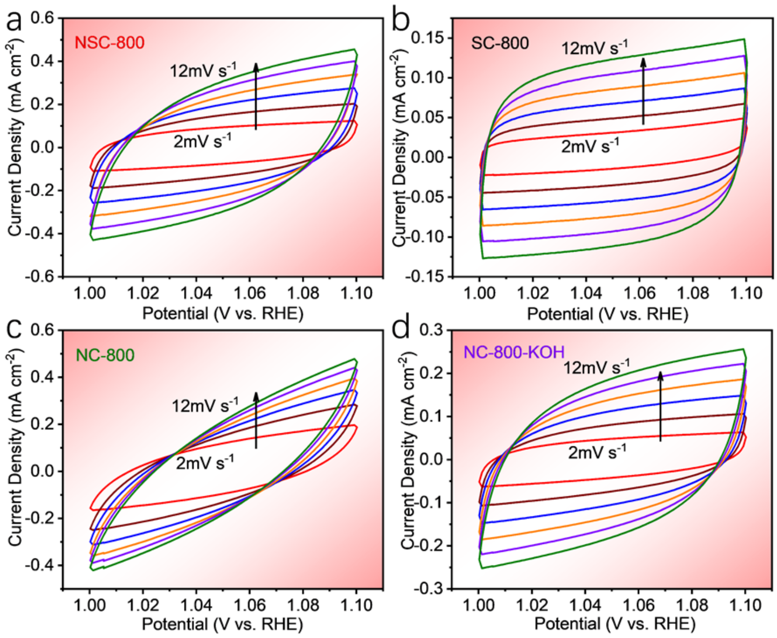

Fig. S6 CV curves in the region of 1.0-1.1 V at scan rates from 2 to 12 mV s^{-1} for (a) NSC-800, (b) SC-800, (c) NC-800, and (d) NC-800-KOH.

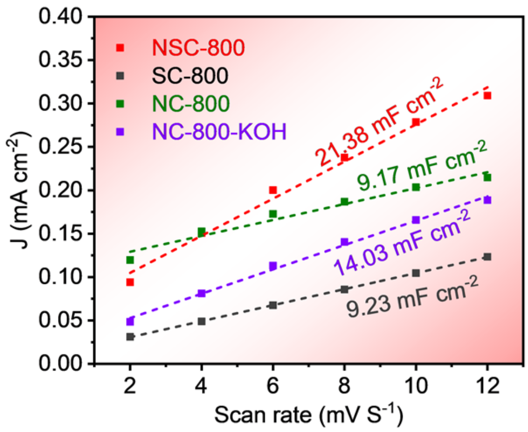

Fig. S7 Linear fitting of capacitive current for NSC-800, SC-800, NC-800 and NC-800-KOH.

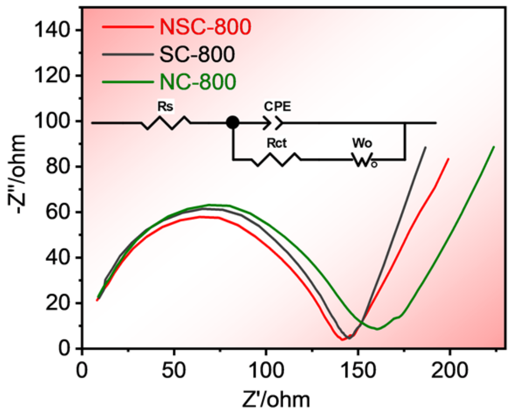

Fig. S8 Nyquist plots of NSC-800, SC-800 and NC-800, with the inset showing the equivalent circuit for fitting the experimental data.

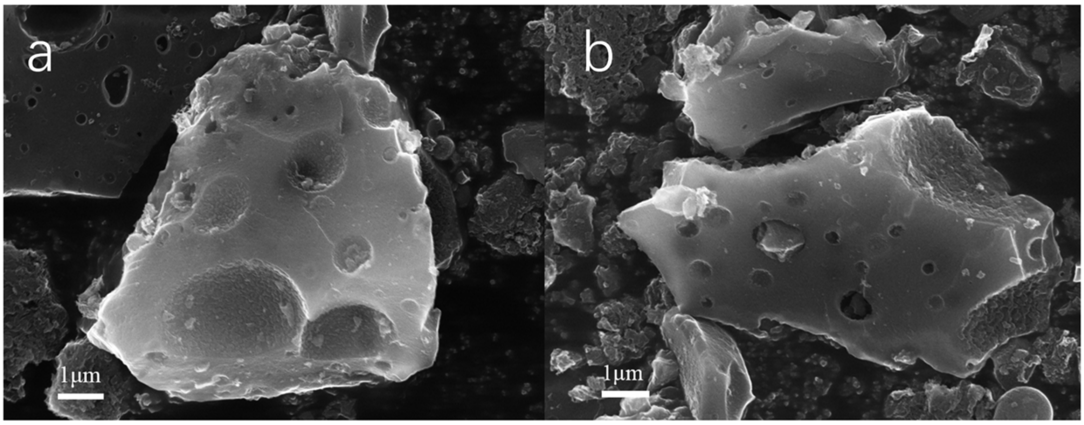

Fig. S9 SEM image of NC-800-KOH

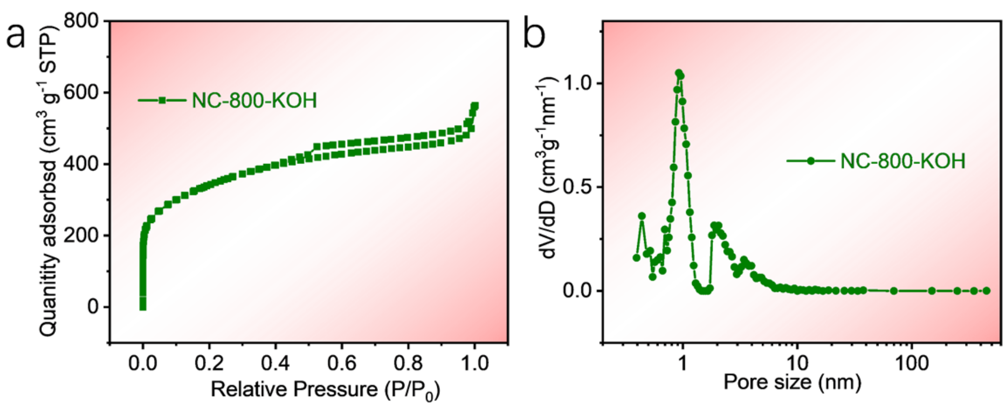

Fig. S10 (a) Nitrogen adsorption and desorption isotherms, and (b) pore size distribution curve of NC-800-KOH

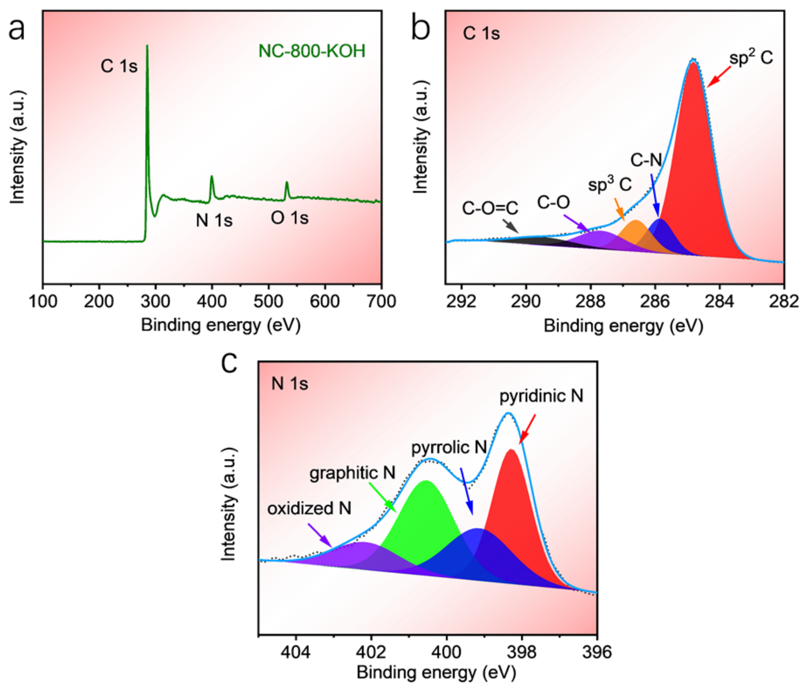

Fig. S11 (a) XPS survey spectra. High-resolution XPS spectra of (b) C 1s and (c) N 1s peaks for NC-800-KOH.

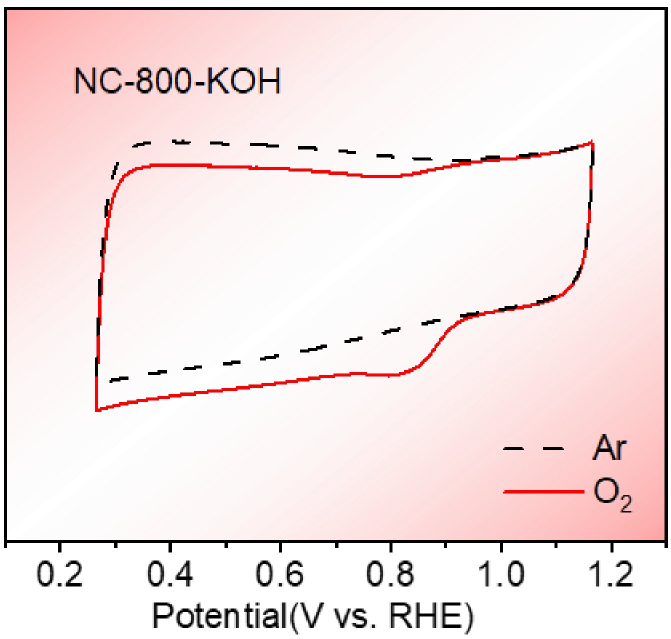

Fig. S12 CV tests for NC-800-KOH under Ar and O_2 saturated 0.1 M KOH.

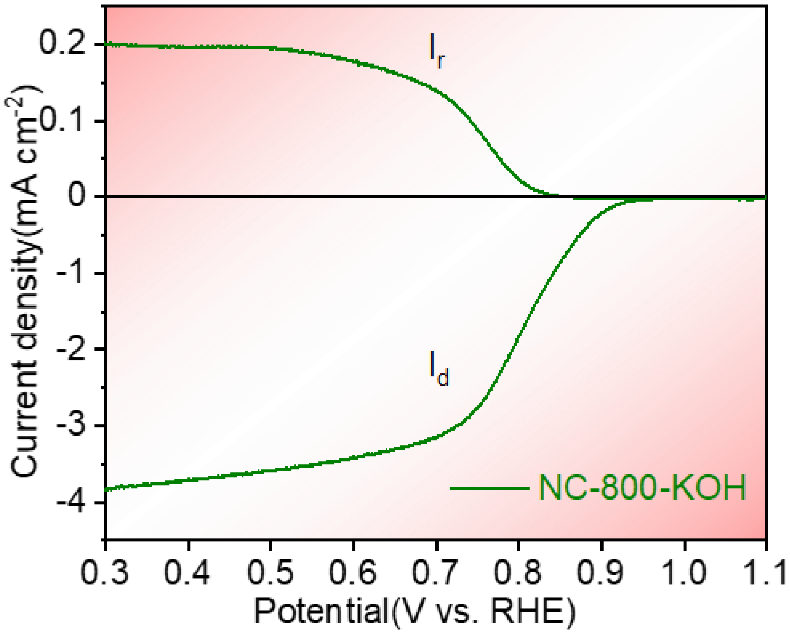

Fig. S13 ORR polarization curves for NC-800-KOH.

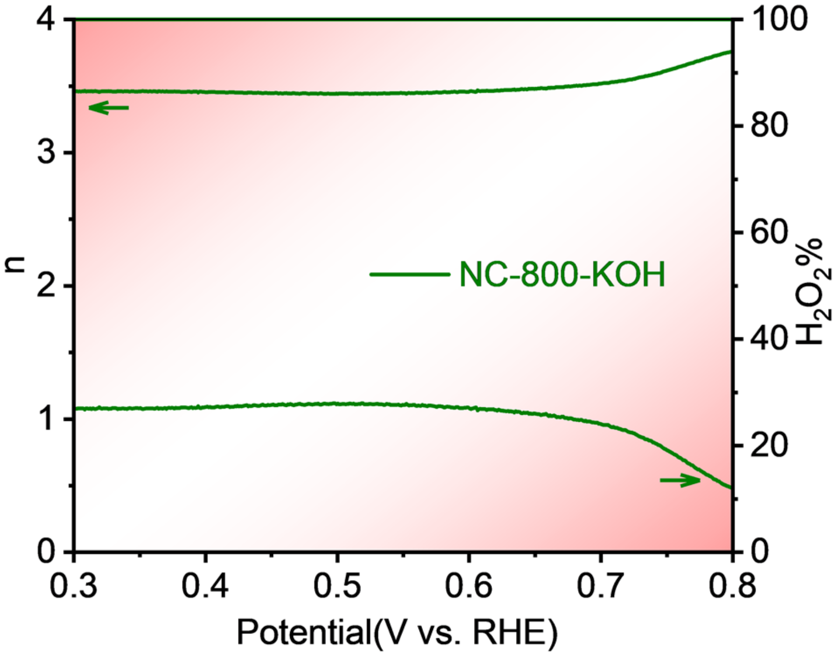

Fig. S14 H_2O_2 yield together with the electron transfer numbers for NC-800-KOH.

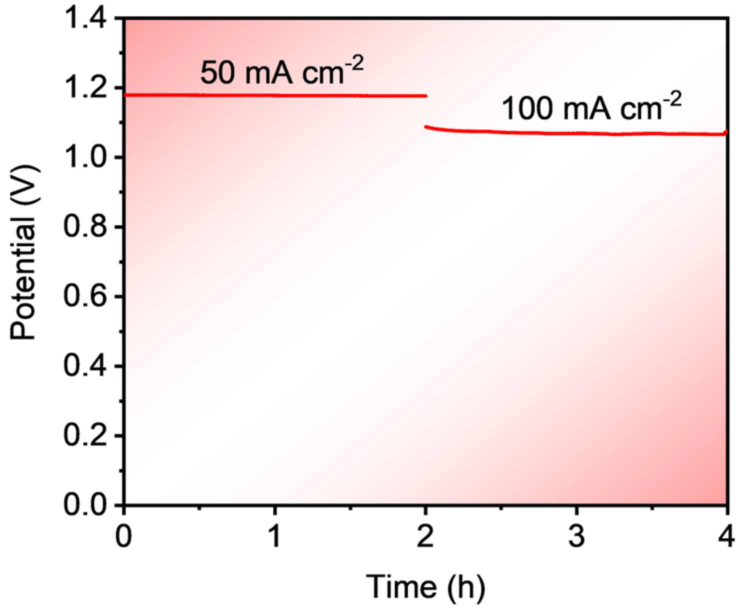

Fig. S15 The galvanostatic discharge-voltage curve of aqueous ZAB with NSC-800 at 50 and 100 mA cm^{-2}.

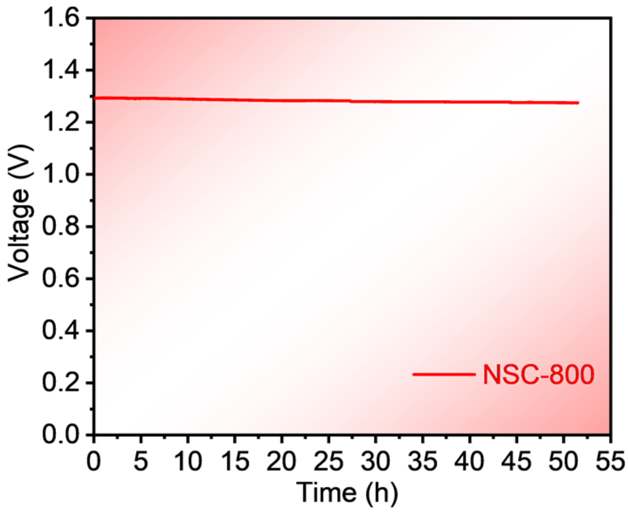

Fig. S16 The galvanostatic discharge-voltage curve of aqueous ZAB with NSC-800 at 10 mA cm^{-2}.

Table S1 Physical properties of NSC-800, SC-800, NC-800 and NC-800-KOH.

sample	S_{BET} (m^2 g^{-1})	V_P (cm^3 g^{-1})	pore volume (%)	
			pore < 2nm	pore > 2nm
NSC-800	1069.4	0.88	63.55	36.45
SC-800	1775.8	2.03	35.70	64.30
NC-800	337.8	0.33	63.23	36.77
NC-800-KOH	1220.3	1.12	41.58	58.42

Table S2 Elemental composition of different samples from XPS spectra.

sample	C */at. %*	N */at. %*	S */at. %*
NSC-800	85.32	8.88	0.57
SC-800	94.10		0.86
NC-800	82.91	10.60	
NC-800-KOH	87.05	8.83	

Table S3 The content of surface carbon species in different samples from high-resolution C1s XPS spectra.

Sample	sp^2 C $/C_{total}$ (%)	sp^3 C $/C_{total}$ (%)	C-N $/C_{total}$ (%)	C-S $/C_{total}$ (%)	C-O $/C_{total}$ (%)	C-O=C $/C_{total}$ (%)
NSC-800	59.88	13.17	10.18	4.79	5.39	6.59
SC-800	66.23	13.25		9.27	3.97	7.28
NC-800	60.24	10.84	12.05		13.25	3.62
NC-800-KOH	67.11	9.40	9.40		8.72	5.37

Table S4 The content of surface nitrogen species in different samples from high-resolution N1s XPS spectra.

Sample	pyridinic-N $/N_{total}$ (%)	pyrrolic-N $/N_{total}$ (%)	graphitic-N $/N_{total}$ (%)	N-oxides $/N_{total}$ (%)
NSC-800	35.69	39.22	18.82	6.27
NC-800	38.61	32.43	21.62	7.34
NC-800-KOH	33.00	33.34	21.67	11.99

Table S5 The content of surface sulfur species in different samples from high-resolution S2p XPS spectra.

Sample	S $2p_{3/2}$ $/S_{total}$ (%)	S $2p_{1/2}$ $/S_{total}$ (%)	S-oxides $/S_{total}$ (%)
NSC-800	57.14	29.14	13.72
SC-800	60.98	31.10	7.92

Table S6 The electrocatalytic activities of the recently reported metal-free and transition-metal catalysts for ORR in the 0.1M KOH solutions.

sample	E_{onset} (V)	$E_{1/2}$ (V)	Ref.
NSC-800	0.980	0.890	This work
CMD-900-4	0.930	0.850	[1]
NVG-30	0.910	0.800	[2]
NBCNT-10	0.958	0.820	[3]
NFPC-1100	0.960	0.850	[4]
$NOPHC_{10}$-900	0.900	0.770	[5]
HPNHC	0.980	0.870	[6]
C_{KI}	0.944	0.828	[7]
N,P-HCNF-8	0.930	0.820	[8]
N-CNSP	0.960	0.850	[9]
N-GPp	0.960	0.830	[10]
h-NCT-900	0.970	0.863	[11]
Fe SA-NSC-900	0.940	0.860	[12]
FeCo-N-HCN	0.980	0.860	[13]
CoN-PCNS	0.930	0.860	[14]

Table S7 EIS spectra fitting results for NSC-800, SC-800 and SC-800.

sample	R_s (Ω cm^{-2})	R_{ct} (Ω cm^{-2})
NSC-800	2.94	130.5
SC-800	3.49	132.4
NC-800	3.01	141.4

Table S8 The OCP and peak power density of the reported Zn-air batteries prepared by the ORR catalyst using liquid alkaline electrolytes.

Electrode material	OCP(V)	Power Density (mW cm^{-2})	Ref.
NSC-800	1.530	166.05	This work
DAP_1-$NDA_{0.5}$-$DBU_{0.5}$	1.480	149.00	[15]
N,P-FC	1.420	148.30	[16]
NPS-G-2	1.372	151.00	[17]
1100-CNS	1.490	151.00	[18]
NFGD	1.180	86.00	[19]
N,P-NC-1000	1.480	146.00	[20]
CoS_x/Co-NC-800	1.400	103.00	[21]
$Fe_{Fe–O–Fe}$-UP/CA	1.490	140.10	[22]
Fe-N-HPC	1.480	164.80	[23]
$4Fe_3O_4$@PCN-800	1.423	156.80	[24]
MNSs@NGA	1.520	115.00	[25]
Fe_3C–FeN/NC-2	1.410	166.00	[26]
g-SA-Mn-900	1.442	147.00	[27]

References

1 Z. Xing, R. Jin, X. Chen, B. Chen, J. Zhou, B. Tian, Y. Li and D. Fan, *Chem. Eng. J.*, 2021, **410**, 128015.

2 Z. Wu, Y. Zhang, L. Li, Y. Zhao, Y. Shen, S. Wang and G. Shao, *J. Mater. Chem. A*, 2020, **8**, 23248-23256.

3 P. Wei, X. Li, Z. He, X. Sun, Q. Liang, Z. Wang, C. Fang, Q. Li, H. Yang, J. Han and Y. Huang, *Chem. Eng. J.*, 2021, **422**, 130134.

4 Y.-N. Sun, J. Yang, X. Ding, W. Ji, A. Jaworski, N. Hedin and B.-H. Han, *Appl. Catal. B: Environ.*, 2021, **297**, 120448.

5 S. Huang, Y. Meng, Y. Cao, S. He, X. Li, S. Tong and M. Wu, *Appl. Catal. B: Environ.*, 2019, **248**, 239-248.

6 Y. Cheng, Y. Wang, Q. Wang, Z. Liao, N. Zhang, Y. Guo and Z. Xiang, *J. Mater. Chem. A*, 2019, **7**, 9831-9836.

7 W.-J. Liu, Y.-Q. Wen, J.-W. Wang, D.-C. Zhong, J.-B. Tan and T.-B. Lu, *J. Mater. Chem. A*, 2019, **7**, 9587-9592.

8 Y. Gao, Z. Xiao, D. Kong, R. Iqbal, Q.-H. Yang and L. Zhi, *Nano Energy*, 2019, **64**, 103879.

9 L. Zong, W. Wu, S. Liu, H. Yin, Y. Chen, C. Liu, K. Fan, X. Zhao, X. Chen, F. Wang, Y. Yang, L. Wang and S. Feng, *Energy Storage Mater.*, 2020, **27**, 514-521.

10 N. Komba, Q. Wei, G. Zhang, F. Rosei and S. Sun, *Appl. Catal. B: Environ.*, 2019, **243**, 373-380.

11 L. Zhao, X.-L. Sui, Q.-Y. Zhou, J.-Z. Li, J.-J. Zhang, G.-S. Huang and Z.-B. Wang, *J. Mater. Chem. A*, 2018, **6**, 6212-6219.

12 M. Wang, W. Yang, X. Li, Y. Xu, L. Zheng, C. Su and B. Liu, *ACS Energy Lett.*, 2021, **6**, 379-386.

13 H. Li, Y. Wen, M. Jiang, Y. Yao, H. Zhou, Z. Huang, J. Li, S. Jiao, Y. Kuang and S. Luo, *Adv. Funct. Mater.*, 2021, **31**, 2011289.

14 Y. Chen, X. Li, W. Liao, L. Qiu, H. Yang, L. Yao and L. Deng, *J. Mater. Chem. A*, 2021, **9**, 3398-3408.

15 D. Lyu, S. Yao, Y. Bahari, S. W. Hasan, C. Pan, X. Zhang, F. Yu, Z. Q. Tian and P. K. Shen, *Appl. Mater. Today*, 2020, **20**, 100737.

16 X. Xue, H. Yang, T. Yang, P. Yuan, Q. Li, S. Mu, X. Zheng, L. Chi, J. Zhu, Y. Li, J. Zhang and Q. Xu, *J. Mater. Chem. A*, 2019, **7**, 15271-15277.

17 X. Zheng, J. Wu, X. Cao, J. Abbott, C. Jin, H. Wang, P. Strasser, R. Yang, X. Chen and G. Wu, *Appl. Catal. B: Environ.*, 2019, **241**, 442-451.

18 Z. Pei, H. Li, Y. Huang, Q. Xue, Y. Huang, M. Zhu, Z. Wang and C. Zhi, *Energy Environ. Sci.*, 2017, **10**, 742-749.

19 S. Zhang, Y. Cai, H. He, Y. Zhang, R. Liu, H. Cao, M. Wang, J. Liu, G. Zhang, Y. Li, H. Liu and B. Li, *J. Mater. Chem. A*, 2016, **4**, 4738-4744.

20 H. Luo, W.-J. Jiang, Y. Zhang, S. Niu, T. Tang, L.-B. Huang, Y.-Y. Chen, Z. Wei and J.-S. Hu, *Carbon*, 2018, **128**, 97-105.

21 Q. Lu, J. Yu, X. Zou, K. Liao, P. Tan, W. Zhou, M. Ni and Z. Shao, *Adv. Funct.*

Mater., 2019, **29**, 1904481.

22 J. Shi, X. Shu, C. Xiang, H. Li, Y. Li, W. Du, P. An, H. Tian, J. Zhang and H. Xia, *J. Mater. Chem. A*, 2021, **9**, 6861-6871.

23 D. Wang, H. Xu, P. Yang, L. Xiao, L. Du, X. Lu, R. Li, J. Zhang and M. An, *J. Mater. Chem. A*, 2021, **9**, 9761-9770.

24 H.-M. Zhang, Y. Zhao, Y. Zhang, M. Zhang, M. Cheng, J. Yu, H. Liu, M. Ji, C. Zhu and J. Xu, *Chem. Eng. J.*, 2019, **375**, 122058.

25 H. Zhao, R. Jiang, Y. Zhang, B. Xie, J. Fu, X. Yuan, W. Yang, Y. Wu and R. Zhang, *J. Mater. Chem. A*, 2021, **9**, 5848-5856.

26 F. Zhou, P. Yu, F. Sun, G. Zhang, X. Liu and L. Wang, *J. Mater. Chem. A*, 2021, **9**, 6831-6840.

27 Q. Zhou, J. Cai, Z. Zhang, R. Gao, B. Chen, G. Wen, L. Zhao, Y. Deng, H. Dou, X. Gong, Y. Zhang, Y. Hu, A. Yu, X. Sui, Z. Wang and Z. Chen, *Small Methods*, 2021, **5**, 2100024.